

Cite this: *RSC Adv.*, 2014, **4**, 3461

The photophysics of 7-(diethylamino)coumarin-3-carboxylic acid *N*-succinimidyl ester in reverse micelle: excitation wavelength dependent dynamics[†]

Banibrata Maity, Aninda Chatterjee and Debabrata Seth*

This paper focuses on the photophysical studies of 7-(diethylamino)coumarin-3-carboxylic acid *N*-succinimidyl ester (7-DCCAЕ) in aqueous reverse micelles using steady state absorption, fluorescence emission and picosecond time resolved emission spectroscopy. We used sodium dioctylsulfosuccinate (AOT) as surfactant to prepare reverse micelles. We have observed excitation wavelength dependent photophysics of 7-DCCAЕ in the reverse micelles. The red edge excitation shift (REES) was found in the reverse micelles, at different w_0 values. The REES gradually decreases with increase in size of the water pool. The rotational relaxation time of the dye molecule decreases with increasing the mole ratio of water to surfactant (w_0) inside the reverse micelles. The fluorescence anisotropy decays were found biexponential in nature with fast and slow reorientation times, which is explained by two steps and "wobbling-in-cone model". We have observed the excitation wavelength dependent dynamics of 7-DCCAЕ in the reverse micelles. We have observed the difference in the photophysics 7-DCCAЕ with its acid form.

Received 7th August 2013
Accepted 22nd October 2013

DOI: 10.1039/c3ra44240c
www.rsc.org/advances

1. Introduction

Reverse micelles are used as template for bio-mimicking media. It is a microheterogeneous system, and used as effective stabilisers for nanomaterials, biological membrane, drug-delivery systems, and have diverse applications.^{1–7} The most important feature of this system is its ability to encapsulate a fairly large amount of water molecules in the core of the reverse micelles.⁸ Reverse micelles are composed of spherical aggregation of surfactant molecules sequestered in non-polar solvents with their polar head groups on the interior, and the non-polar hydrophobic hydrocarbon tails projecting outward into non-polar solvents. The interaction between the polar headgroups of the surfactant with water molecules creates a confined liquid phase. This forms a well-defined nanometer sized "water-pool".⁹ It is termed as "nano beakers",¹⁰ here reaction occurs by the micelles exchange reactants phenomenon. These confined systems can simplify many chemical and physical processes. Such nanometer sized water pool is characterised by several techniques.^{10–18} The size of the "water-pool" is controlled by w_0 ($w_0 = [\text{water}]/[\text{surfactant}]$).

The water molecule entrapped in the water pool behaves differently compared to the bulk water. Several reports are available in the literature which describe that the water molecule plays an important role in biological systems.^{10–18} The dynamics of water molecules in the water pool of reverse micelles are different as compared to neat water. In neat water solvent relaxation is very fast,¹⁹ whereas in reverse micelles, the solvent relaxations are retarded several times as compared to neat water.^{9,20–25} We have used Aerosol-OT [AOT, sodium di(2-ethylhexyl) sulfosuccinate] to prepare reverse micelles.

Coumarins have a potential application in biomedical analysis,²⁶ pharmaceutical industry,²⁷ extensively metabolized properties,²⁸ drug delivery system,²⁹ laser dyes in the blue-green region^{30,31} and used as optical chromophores³² in homogeneous as well as in biomimicking media. Aminocoumarin derivatives have drawn much more attention in the last few decades. 7-Aminocoumarin can be regarded as a strong fluorescence probe due to the presence of an electron donating and accepting part, which influences the transfer of electron through the bond joining them and involves complete charge transfer as well as twisting. As a result, a twisted intramolecular charge transfer (TICT) state is formed, in which the donor orbitals are orthogonal to the acceptor orbital. This process is strongly dependent on the polarity and viscosity of the medium. Upon photoexcitation, these dyes undergo a large Stokes shift as well as a substantial change in the dipole moment between ground and excited state.^{33,34}

Department of Chemistry, Indian Institute of Technology, Patna 800013, Bihar, India.
E-mail: debabrata@iitp.ac.in; Fax: +91-612-2277383

† Electronic supplementary information (ESI) available. See DOI: [10.1039/c3ra44240c](https://doi.org/10.1039/c3ra44240c)

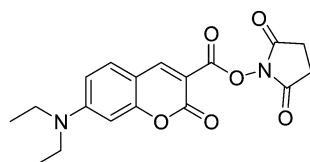


With this in mind, our special interest concerns the photophysical investigation of 7-(diethylamino)coumarin-3-carboxylic acid *N*-succinimidyl ester (7-DCCAE) in the presence of water reverse micelles. The structure of 7-DCCAE is quite hydrophobic in nature, may be applied to label the cells^{35,36} and has an important application for generating blue-fluorescent bioconjugates.^{35,36} The probe molecule has a significant role in the ascertainment of amino acids by capillary zone electrophoresis based on semiconductor laser fluorescence detection.³⁷ The structure of this coumarin is resembling 7-(diethylamino)coumarin-3-carboxylic acid (7-DCCA) and in accordance with another well studied probe Coumarin-343 (C-343). In 7-DCCAE, an acidic hydrogen atom of 7-DCCA is replaced by *N*-succinimidyl ester moiety to make the molecule quite hydrophobic. To get an idea of the fluorescent behaviour of this molecule in the biological system we have studied the photodynamics of 7-DCCAE in confined media, such as reverse micelles. The chemistry in confined media mimics the extremely efficient chemical or biological processes occurring in nature.³⁸ The photophysical properties of coumarin dyes in different confined media such as cyclodextrins, micelles and reverse micelles have been reported in the literature.^{19–25,39–49} To know the effect of confinement on the photodynamics of 7-DCCAE we have used isoctane/AOT/water reverse micelles. In isoctane/AOT/water reverse micelles we have studied the photophysics of 7-DCCAE by varying the excitation wavelength. To the best of our knowledge this is the first report of the dynamics of 7-DCCAE in confined media.

2. Experimental and methods

7-(Diethylamino)coumarin-3-carboxylic acid *N*-succinimidyl ester (7-DCCAE, Scheme 1) was purchased from Sigma-Aldrich and used as received. Sodium dioctylsulfosuccinate (AOT) was purchased from Sigma-Aldrich. AOT was dried under vacuum and used as described in literature.⁴⁹ The concentration of AOT was maintained as 0.1 (M) for all measurements. Reverse micelles are formed by adding the required amount of water in an isoctane–AOT mixture at different w_0 values, where $w_0 = [\text{water}]/[\text{AOT}]$. Millipore water was used for all measurements. The concentration of 7-DCCAE was maintained as 3×10^{-6} M for all measurements.

Steady state UV-Vis absorption measurements were carried out using Shimadzu UV-Vis spectrophotometer (model: UV-2550). Steady state fluorescence emission measurements were carried out using Horiba Jobin Yvon spectrofluorometer (model: Fluoromax-4P). For all steady state absorption and fluorescence measurements the temperature was kept constant



Scheme 1 Schematic representation of 7-DCCAE.

at 298 K using Jeiotech refrigerated bath circulator (model: RW0525G). The fluorescence quantum yield of coumarin 480 in water solution ($\phi_f = 0.66$)³⁴ was used as a reference to measure the fluorescence quantum yields of 7-DCCAE in all systems. The following equation was used to calculate the fluorescence quantum yield of 7-DCCAE:

$$\phi_s = \phi_r \frac{I_s A_r n_s^2}{I_r A_s n_r^2} \quad (1)$$

where ϕ_r is the fluorescence quantum yield of reference. I stands for the integrated area under the emission curves. The subscripts s and r stand for sample and reference, respectively. A is the absorbance at a particular excitation wavelength. n is the refractive index of the medium. The absorbance of the dye at the excitation wavelength was always kept ~ 0.1 . The steady state absorption and emission spectra were fitted by the log normal line shape function, which is defined as:

$$I(\nu) = I_0 \exp \left[-\ln 2 \left(\frac{\ln [1 + 2b(\nu - \nu_p)/\Delta]}{b} \right)^2 \right] \quad (2)$$

where ν_p , I_0 , Δ , and b are the peak frequency, peak height, width parameter, and asymmetric parameter, respectively. All fluorescence spectra were scaled by a λ^2 factor prior to the lognormal fitting of the respective spectra to obtain the mean frequencies.⁵⁰

The picosecond time-correlated single-photon counting (TCSPC) technique was used to measure the fluorescence time resolved decays. We have used time-resolved fluorescence spectrophotometer from Edinburgh Instruments (model: LifeSpec-II, UK). We have used picosecond diode lasers at 375, 405 and 445 nm as an excitation source. The instrument response function (IRF) of our system is ~ 80 ps. The fluorescence decays were detected at the magic angle (54.7°) polarization using Hamamatsu MCP PMT (3809U) as detector. The decays were analysed using F-900 decay analysis software. The fluorescence anisotropy decays $r(t)$ were measured using the same instrument. The following equation was used to get $r(t)$.

$$r(t) = \frac{I_{\parallel}(t) - GI_{\perp}(t)}{I_{\parallel}(t) + 2GI_{\perp}(t)} \quad (3)$$

To measure the anisotropy decay, the emission intensities at parallel (I_{\parallel}) and perpendicular (I_{\perp}) polarizations were collected alternatively by fixing the time for both decays. We have used motorised polarizers to collect the parallel and perpendicular decays. G is the correction factor for the detector sensitivity to the polarization direction of the emission. $G = I_{\text{HV}}/I_{\text{HH}}$, where I_{HV} and I_{HH} are the sensitivities of the emission part of the instrument for the vertical and horizontal polarized components. A similar method was used to measure the G factor. F-900 software was used to analyze the anisotropy decay. For all time resolved measurements the temperature was kept constant at 298 K using Peltier-controlled cuvette holders from the Quantum Northwest (model: TLC-50).

The anisotropy decays are best fitted by a biexponential function which consists of both the slow and fast components.

$$\langle \tau_{\text{rot}} \rangle = \beta \tau_{\text{slow}} + (1 - \beta) \tau_{\text{fast}} \quad (4)$$

where τ_{slow} and τ_{fast} are the two time constants associated with the decays of the probe molecule anisotropy inside the reverse micelles. β is the percentage contribution of the slow component, whereas $(1 - \beta)$ is the relative percentage contribution of the fast component. This biexponential nature of the anisotropy decay in reverse micelles was explained by two steps and a wobbling-in-cone model^{51–59} which consists of wobbling (rotational) and translational diffusion of the molecule coupled with rotational motion of the micelle as a whole. According to this model, the observed slow rotational relaxation is a convolution of the relaxation time corresponding to the overall rotation of the micelles (τ_M) and the lateral diffusion of the probe (τ_L) inside the reverse micelles. Additionally, the wobbling-in-cone model also describes the internal motion of the probe (τ_w) in terms of cone angle (θ) and wobbling diffusion coefficient (D_w).

$$\frac{1}{\tau_{\text{slow}}} = \frac{1}{\tau_M} + \frac{1}{\tau_L} \quad (5)$$

$$\frac{1}{\tau_{\text{fast}}} = \frac{1}{\tau_w} + \frac{1}{\tau_{\text{slow}}} \quad (6)$$

The overall rotation of the micelles (τ_M) can be calculated using the Debye–Stokes–Einstein (DSE) relation with the stick boundary condition:

$$\tau_M = \frac{4\pi\eta r_h^3}{3kT} \quad (7)$$

where η is the viscosity of isoctane, r_h is the hydrodynamic radius of the AOT reverse micelles. k and T are the Boltzmann constant and the absolute temperature, respectively. The hydrodynamic radius (r_h) of the AOT reverse micelles is given by the following equation^{58,59}

$$r_h = 0.5d_{\text{wp}} + 1.0 \text{ nm} \quad (8)$$

d_{wp} is the diameter of the water pool inside the isoctane/water/AOT reverse micelles. Again, d_{wp} is known as^{58,59}

$$d_{\text{wp}} = 0.29w + 1.1 \text{ nm.} \quad (9)$$

The translational (lateral) diffusion coefficient of the probe is related to τ_L as follow:

$$D_L = \frac{r_h^2}{6\tau_L}. \quad (10)$$

We have estimated the order parameters (S) to determine the location as well as the spatial restriction imposed by the solvent molecules on the probe.

$$\beta = S^2 \quad (11)$$

where S is the square of the order parameter, which is a measure of the equilibrium orientation distribution of the probe molecule, β is the pre-exponential factor for the slow component of rotational relaxation. We have also determined the cone angle (θ) and the wobbling diffusion coefficient (D_w) as follows:

$$\theta = \cos^{-1} \left[\frac{1}{2} \left((1 + 8S)^{\frac{1}{2}} - 1 \right) \right] \quad (12)$$

$$D_w \tau_w (1 - S^2) = \frac{-x_0^2 (1 + x_0)^2 \{ \ln[(1 + x_0)/2] + (1 - x_0)/2 \}}{2(1 - x_0)} + \frac{(1 - x_0)}{24} (6 + 8x_0 - x_0^2 - 12x_0^3 - 7x_0^4). \quad (13)$$

θ is the cone angle in radians.

3. Results and discussion

The photophysical properties of 7-DCCA were studied in isoctane/water/AOT reverse micelles. We have compared our results on 7-DCCA with the photophysics of its analogue molecule 7-(diethylamino)coumarin-3-carboxylic acid (7-DCCA). The photophysics of 7-DCCA were reported earlier.^{25,41}

3.1. Steady state absorption and emission spectral studies in aqueous reverse micelles

7-DCCA showed an absorption peak at 444 nm in water, whereas its analogue molecule 7-DCCA showed an absorption peak at 408 nm in water. In the isoctane–AOT mixture ($w_0 = 0$) 7-DCCA showed an absorption peak at 420 nm. With the addition of water the absorption peak was gradually red shifted. At $w_0 = 30$ the absorption peak of 7-DCCA was found at 431 nm. The change in the absorption peak of 7-DCCA in isoctane/water/AOT reverse micelles is shown in Fig. 1(a). The absorption peak of 7-DCCA at higher w_0 is blue shifted as compared to bulk water. In the case of 7-DCCA the absorption peak also undergoes a red shift from 387 nm (at $w_0 = 0$) to 406 nm (at $w_0 = 30$) in the presence of isoctane/water/AOT reverse micelles.²⁵

The fluorescence emission peak of 7-DCCA was observed at 477 nm in water. The emission peak of 7-DCCA in water was observed at 473 nm. We have studied the excitation wavelength dependent fluorescence emission properties of 7-DCCA in reverse micelles. In an isoctane–AOT mixture ($w_0 = 0$) 7-DCCA showed an emission peak at 440, 444 and 459 nm, when the excitation wavelengths (λ_{exi}) are 375, 405 and 445 nm respectively. With gradual addition of water in the isoctane–AOT mixture, the fluorescence emission peak of 7-DCCA shifted to red. This is due to the migration of the dye molecule to the centre of the water pool from the interface region. We have observed the excitation wavelength dependent fluorescence emission peak in all w_0 values. Even at $w_0 = 30$ we have observed a change in the emission peak of 7-DCCA with the excitation wavelength. The emission peak positions of 7-DCCA in reverse micelles at different w_0 values are tabulated in Table 1 and shown in Fig. 1(b) and (c) respectively. With the gradual increase of w_0 value, the emission peak position changes from 440 nm (at $w_0 = 0$) to 456 nm ($w_0 = 30$) when $\lambda_{\text{exi}} = 375$ nm. For $\lambda_{\text{exi}} = 405$ nm, the fluorescence emission peak position changes from 444 to 457 nm (from $w_0 = 0$ to 30). A similar trend was also



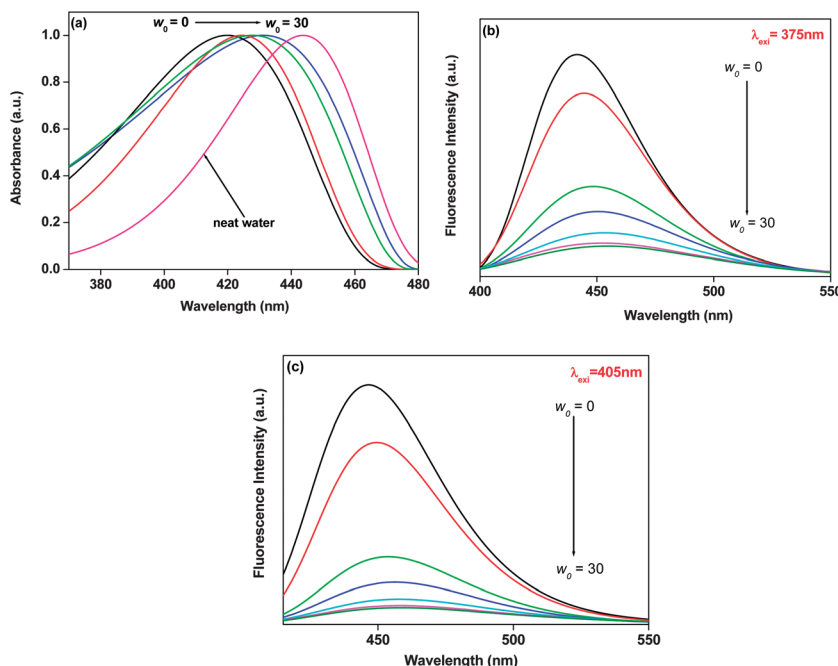


Fig. 1 (a) Change in the absorption spectral position of 7-DCCA in isooctane/water/AOT reverse micelles at different w_0 values and in neat water. (b) Fluorescence emission spectral shift positions when $\lambda_{\text{exi}} = 375$ nm and (c) $\lambda_{\text{exi}} = 405$ nm of 7-DCCA in isooctane/water/AOT reverse micelle.

observed at $\lambda_{\text{exi}} = 445$ nm, where the emission peak position shifts from 459 to 474 nm (from $w_0 = 0$ to 30). We also found that the fluorescence quantum yield (ϕ_f) gradually decreases with increase of the w_0 value at different excitation wavelengths ($\lambda_{\text{exi}} = 375, 405$ and 445 nm). Similar results were observed in

the case of 7-DCCA molecule,²⁵ where we used 375 and 405 nm lasers as the excitation wavelength. Likewise, for 7-DCCA,²⁵ here 7-DCCA in water faces a less polar environment inside the reverse micelles as compared to bulk water. In Fig. 2(a) we have shown a change in the emission peak as a function of the

Table 1 Fluorescence emission parameters of 7-DCCA in isooctane/water/AOT reverse micelles

System	w_0	λ_{exi} (nm)	ϕ_f^a	$\lambda_{\text{max}}^{\text{abs}}$ (nm)	$\lambda_{\text{max}}^{\text{emi}}$ (nm)	$\tau_f^{a,b}$ (ns)	k_r^a ($\times 10^9$) s^{-1}	k_{nr}^a ($\times 10^9$) s^{-1}
7-DCCA in isoctane/water/AOT reverse micelles	0	375	0.511	420	440	2.390	0.214	0.21
	1		0.446	421	442	1.367	0.326	0.41
	3		0.311	424	446	1.301	0.239	0.53
	5		0.146	425	448	1.083	0.135	0.79
	10		0.100	428	452	0.907	0.110	0.99
	20		0.084	429	453	0.849	0.099	1.08
	30		0.071	431	456	0.831	0.085	1.12
7-DCCA in water	—	0.010	444	477	0.045	0.222	22.0	
7-DCCA in isoctane/water/AOT reverse micelles	0	405	0.601	420	444	2.432	0.247	0.16
	1		0.437	421	447	2.120	0.206	0.27
	3		0.192	424	451	1.221	0.157	0.66
	5		0.112	425	454	0.675	0.166	1.32
	10		0.074	428	455	0.504	0.147	1.84
	20		0.059	429	456	0.453	0.130	2.08
	30		0.053	431	457	0.436	0.122	2.17
7-DCCA in isoctane/water/AOT reverse micelles	0	445	0.491	420	459	2.118	0.232	0.24
	1		0.403	421	460	1.545	0.261	0.39
	3		0.200	424	464	0.613	0.326	1.30
	5		0.104	425	467	0.351	0.296	2.55
	10		0.042	428	470	0.215	0.195	4.46
	20		0.028	429	473	0.155	0.180	6.27
	30		0.025	431	474	0.114	0.219	8.55

^a Experimental error of $\pm 5\%$. ^b χ^2 values are under 1.2.



excitation wavelength. We have shown a change in the full width half maxima (FWHM) of 7-DCCA in reverse micelles at different w_0 values in the case of two different excitation wavelengths (shown in Fig. 2(b)). From these figures it is clear that 7-DCCA showed excitation wavelength dependent emission properties in reverse micelles. The excitation spectra of 7-DCCA in reverse micelles are shown in Fig. S1.[†]

The fluorescence emission peak position red shifted with increase in the excitation wavelength. This is known as red-edge excitation shift (REES). This is observed when fluorophores are in viscous or motionally restricted environments. The dipolar relaxation of the solvent molecules becomes slow and comparable to or longer than the fluorescence lifetime decay. In organised assemblies such as proteins, micelles, vesicles, micelles, condensed or frozen medium like low-temperature glasses, polymer matrices *etc.*, the REES are most common and primarily arise because of hydrophilic and hydrophobic pockets of heterogeneity assemblies allow the solvent sites to contribute to inhomogeneous broadening of the absorption spectra.^{60–63} The broadening of the spectra arises due to solute–solvent interaction in the excitation energy states and can be categorised as static and dynamic broadening. In rigid environments when the dipolar relaxation of the solvent molecule around the fluorophore is slower than the rate of emission then it is static broadening. On the other hand, when this motion in the fluorophore environment is comparable to or faster than the rate of emission then it is dynamic broadening.⁶² The origin of REES arises from the slow rates of solvent relaxation around an excited state fluorophore, which reflects the rigidity around the immediate vicinity of the fluorophore. In our case we are unable to detect the solvent relaxation due to the limited time resolution of our setup. Therefore, in our system solvent relaxation is faster as compared to the fluorescence decay time of 7-DCCA. It may be possible that hydrogen bonding between 7-DCCA with the media is the main specific interaction for such kind of REES. Here, the probe molecule 7-DCCA is a hydrogen bond acceptor and the water molecule acts as a hydrogen bond donor. Most recently, we reported that the hydrogen bonding interaction is the main reason between observed REES of 7-DCCA in reverse micelles.²⁵

In this paper, we have observed a red-edge excitation shift (REES) of the 7-DCCA molecule in isoctane/water/AOT reverse micelles at different w_0 values. At $w_0 = 0$ the emission maxima are shifted from 449 to 459 nm. So about 10 nm REES with changing of the excitation wavelength from 423 to 445 nm was observed. With increase of the water content, the extent of REES gradually decreases. The variations of the fluorescence emission peak with change in the excitation wavelengths at different w_0 values are shown in Fig. 3. With increase in the size of the water pool inside the reverse micelles, the number of free water molecules increases. Thereby, the micro-viscosity of the medium gradually decreases on going from $w_0 = 0$ to 30 and the corresponding REES decreases. The change in REES with variation of the w_0 value is shown in Fig. 3(c). In our previous study, we observed that the 7-DCCA molecule also exhibits a red-edge excitation shift (REES) in isoctane/water/AOT reverse micelles. The value of REES is 11 nm at $w_0 = 1$. This value gradually decreases with the increase of w_0 value and at $w_0 = 30$, it becomes only 2 nm.²⁵ Similar results have previously been reported by Chattopadhyay *et al.*, they also observed the REES in isoctane/water/AOT reverse micelles and the value of REES gradually decreases with increase of the w_0 values.⁶⁴

3.2. Time resolved emission studies of 7-DCCA in reverse micelles

The time resolved fluorescence emission decay of 7-DCCA in isoctane/water/AOT reverse micelles at different w_0 values was observed. We observed excitation wavelength dependent fluorescence emission decay of 7-DCCA in reverse micelles. We have studied the fluorescence emission decay using different excitation wavelengths. In all cases we observed that with increase in the w_0 value, the fluorescence lifetime value gradually decreases. We have calculated the radiative and non-radiative decay rate of 7-DCCA in reverse micelles using eqn (4) and (5):

$$k_r = \frac{\phi_f}{\tau_f} \quad (14)$$

$$\frac{1}{\tau_f} = k_r + k_{nr} \quad (15)$$

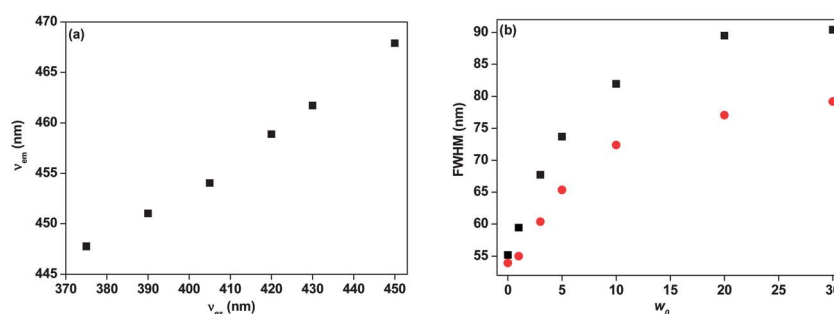


Fig. 2 (a) Change in the fluorescence emission peak positions of 7-DCCA with the change in the excitation wavelengths in isoctane/water/AOT reverse micelle at $w_0 = 5$. (b) Plot of FWHM of the fluorescence emission spectra of 7-DCCA in isoctane/water/AOT reverse micelles at various w_0 values (0 to 30) for (i) $\lambda_{\text{exi}} = 375$ nm (■) and (ii) $\lambda_{\text{exi}} = 405$ nm (●).



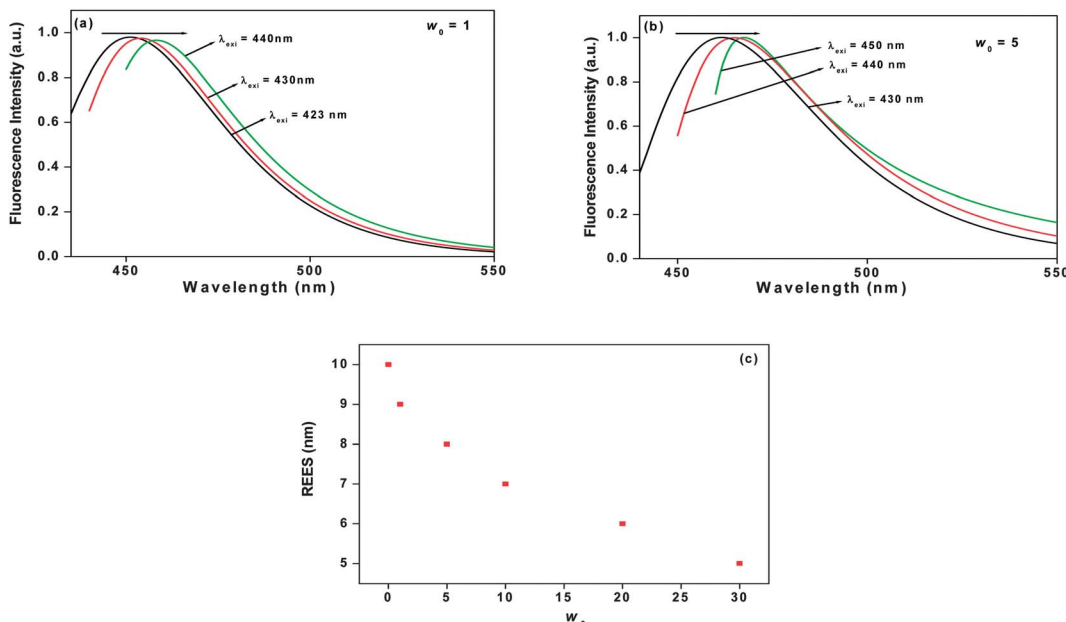


Fig. 3 Change in the emission spectral shift of 7-DCCAЕ with change in the excitation wavelengths at (a) $w_0 = 1$ and (b) $w_0 = 5$. (c) Change in the red-edge excitation shift (REES) of 7-DCCAЕ with variation of w_0 value in isoctane/water/AOT reverse micelles.

k_r is the radiative rate constant and k_{nr} is the non-radiative rate constant. We have observed that with increase in w_0 the k_{nr} values gradually increase. When $\lambda_{exi} = 375$ nm, the k_{nr} value increases ~ 5.5 times ongoing from $w_0 = 0$ to $w_0 = 30$ value. When $\lambda_{exi} = 405$ nm the k_{nr} value increases ~ 13.0 times ongoing from $w_0 = 0$ to $w_0 = 30$ value. When $\lambda_{exi} = 445$ nm, the increment of k_{nr} value is ~ 36 times (from $w_0 = 0$ to 30). From the magnitude of the k_{nr} value and the fluorescence lifetime of 7-DCCAЕ in reverse micelles, excitation wavelength dependency was observed (Table 1). The fluorescence lifetime values of 7-DCCAЕ in reverse micelles at different excitation wavelengths are shown in Fig. 4. Therefore, it is clear that with increase in the water content of the reverse micelles core, the number of free water molecule increases¹⁵ and hence the probe molecule suffers less restricted environment. As a result, the lifetime value gradually decreases and the corresponding non-radiative decay rate constant (k_{nr}) gradually increases with the increase of the w_0 values and hence the TICT process becomes much more favourable. We also found the same effects of its analogue probe 7-DCCA molecule in isoctane/water/AOT reverse micelles.²⁵

3.3. Rotational relaxation studies

The rotational reorientation dynamics of 7-DCCAЕ has been investigated in isoctane/water/AOT reverse micelles using picosecond time-resolved emission spectroscopy. The fluorescence anisotropy decays have been collectively measured by exciting at different wavelengths ($\lambda_{exi} = 375, 405$ and 445 nm) as tabulated in Table 2. The average rotational relaxation time (τ_{rot}) becomes faster at higher w_0 in all cases. We observed that when $\lambda_{exi} = 375$ nm, τ_{rot} value decrease ~ 3 times ongoing from $w_0 = 0$ to $w_0 = 30$ value whereas, if $\lambda_{exi} = 405$ nm, τ_{rot} value decrease ~ 3.5 times (from $w_0 = 0$ to 30). In case of $\lambda_{exi} =$

445 nm, the rotational relaxation time gradually decreases with increase in w_0 value and becomes fast. At $w_0 = 3$, the rotational relaxation time is 2.64 ns, whereas for $w_0 = 20$, this value becomes 1.61 ns. Interestingly, at $w_0 = 30$, we have noticed a “dip–rise–dip” nature of the profile in a fluorescence anisotropy decay (shown in Fig. S2†). This can be ascribed as the non-radiative decay rate constant increases in a greater extent and the corresponding fluorescence lifetime value decreases. This kind of “dip–rise–dip” features are also found in the literature.^{65,66} The anisotropy results are tabulated in Table 2 and the biexponential fitted curves are also shown in Fig. 5. Exploration of Table 2 reveals that at higher w_0 values, the slow component (τ_{slow}) and its relative percentage decreases, whereas the value of the fast component (τ_{fast}) decreases, but its relative percentage increases. This can be ascribed to the fact that the dye molecule experiences less restricted environment with increasing the micelle size. This biexponential nature of anisotropy decay in reverse micelles is neither due to the anisotropic rotation of the probe molecule nor due to two different locations of the probe in the micelle. The rotational relaxation of the dye 7-DCCAЕ is due to the different types of the motion of the fluorophore inside the reverse micelle. The biexponential nature of the anisotropy decay was explained by two steps and the wobbling-in-cone model^{51–59} which consist of wobbling (rotational) and translational diffusion of the molecule coupled with rotational motion of the micelle as a whole. According to this model, the overall rotation of the micelles (τ_M) and the lateral diffusion of the probe (τ_L) inside the reverse micelles, the internal motion of the probe (τ_w) was calculated using different relations as described in the Experimental section (Table 3). The value of the order parameter (S) lies within the range $0 \leq S^2 \leq 1$. $S = 0$ indicates an unrestricted rotation of the probe and $S = 1$ a



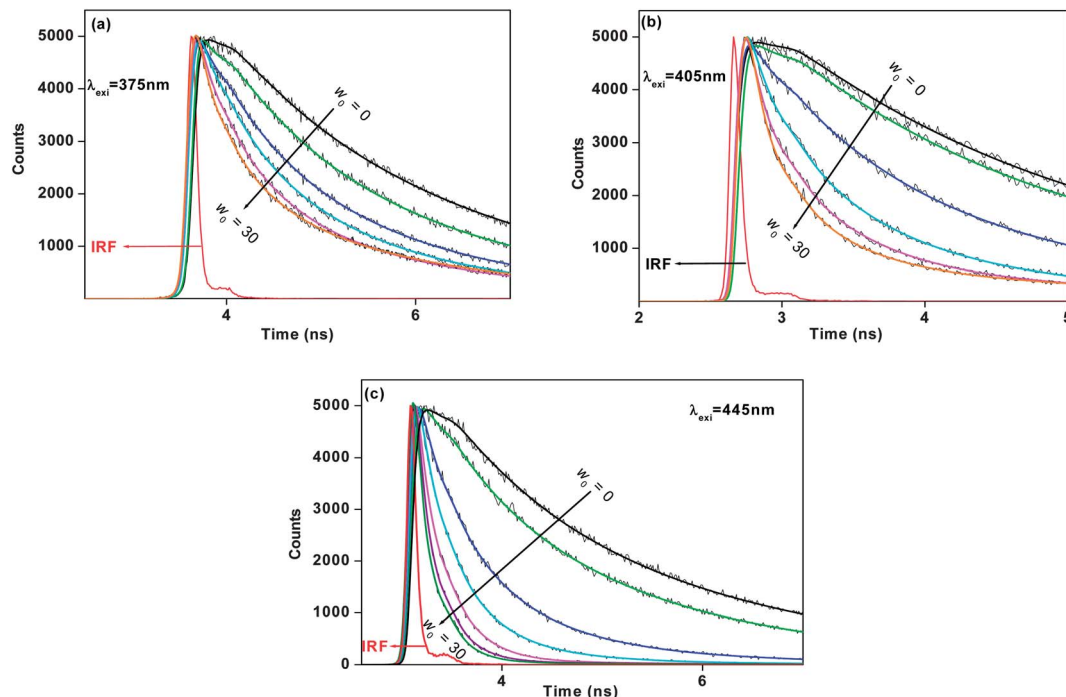


Fig. 4 Fluorescence lifetime decays of 7-DCCAE in isoctane/water/AOT reverse micelles at different w_0 values for (a) $\lambda_{\text{exi}} = 375$ nm, (b) $\lambda_{\text{exi}} = 405$ nm, and (c) $\lambda_{\text{exi}} = 445$ nm.

completely restricted motion. The value of S decreases with increasing the w_0 value, when $\lambda_{\text{exi}} = 375$ and 405 nm (Table 3). This is due to the fact that with gradual swelling of the reverse micelles, the restriction on the rotational motion of the dye decreases. When $\lambda_{\text{exi}} = 445$ nm, the value of S is close to 1, it implies that the motion of the molecules is highly restricted

(Table 3). We have determined the cone angle (θ) and the wobbling diffusion coefficient (D_w) using eqn (12) and (13). All parameters involved in the wobbling-in-cone model are tabulated in Table 3. The obtained parameters indicate that the value of S decreases and the corresponding cone angle (θ) increases with increasing the w_0 value when $\lambda_{\text{exi}} = 375$ and 405

Table 2 Rotational relaxation time of 7-DCCAE in isoctane/water/AOT reverse micelles^a

Sr no.	System	w_0	λ_{exi} (nm)	r_0	τ_1 (ns)	a_1	τ_2 (ns)	a_2	$\langle \tau \rangle_{\text{rot}}^b$ (ns)
1.	7-DCCAE in isoctane/water/AOT reverse micelles	0	375	0.32	0.15	0.21	1.76	0.79	1.42
2.		1		0.30	0.33	0.20	2.23	0.80	1.85
3.		3		0.29	0.21	0.30	1.70	0.70	1.25
4.		5		0.31	0.24	0.39	1.46	0.61	0.98
5.		10		0.31	0.16	0.37	0.90	0.63	0.63
6.		20		0.29	0.23	0.51	0.81	0.49	0.51
7.		30		0.30	0.17	0.49	0.76	0.51	0.47
8.	7-DCCAE in isoctane/water/AOT reverse micelles	0	405	0.34	0.23	0.05	1.85	0.95	1.77
9.		1		0.33	0.76	0.17	2.31	0.83	2.05
10.		3		0.36	0.21	0.16	2.30	0.84	1.97
11.		5		0.32	0.14	0.12	1.29	0.88	1.15
12.		10		0.30	0.11	0.17	0.98	0.83	0.83
13.		20		0.32	0.10	0.25	0.72	0.75	0.57
14.		30		0.35	0.09	0.28	0.66	0.72	0.50
15.	7-DCCAE in isoctane/water/AOT reverse micelles	0	445	0.33	0.06	0.02	1.87	0.98	1.83
16.		1		0.38	0.04	0.11	2.21	0.89	1.97
17.		3		0.35	0.09	0.02	2.69	0.98	2.64
18.		5		0.35	0.07	0.07	2.37	0.93	2.21
19.		10		0.32	0.06	0.07	1.92	0.93	1.79
20.		20		0.29	0.04	0.01	1.63	0.99	1.61

^a Experimental error of $\pm 5\%$. $\langle \tau \rangle_{\text{rot}} = a_1 \tau_1 + a_2 \tau_2 + a_3 \tau_3$. ^b χ^2 values are under 1.2.



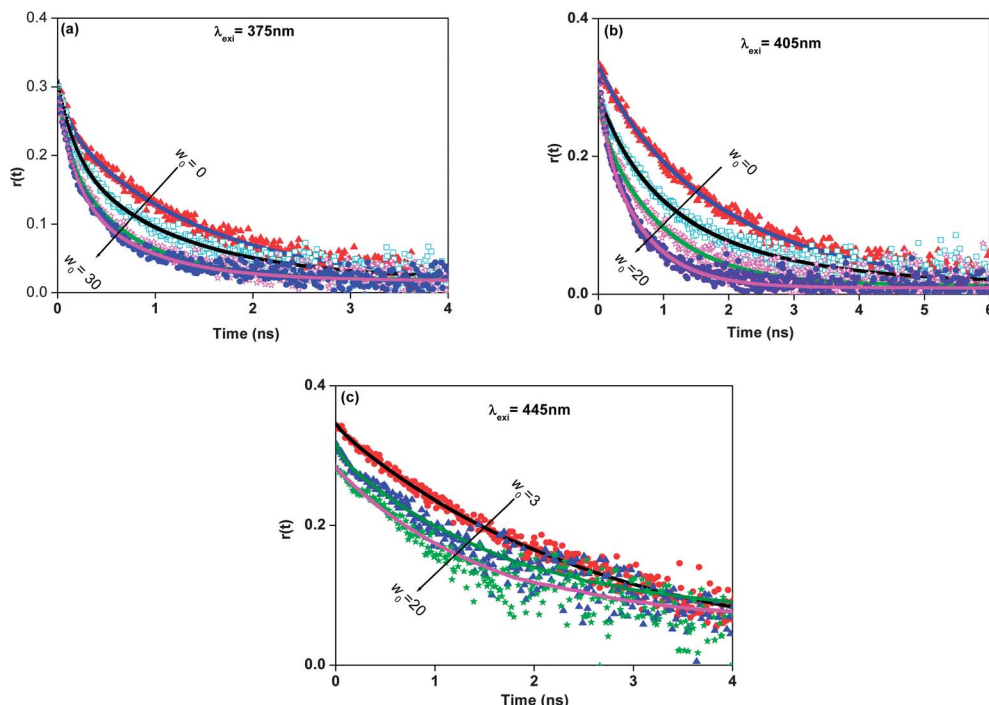


Fig. 5 Time resolved anisotropy decays of 7-DCCAE in isoctane/water/AOT reverse micelles at different w_0 values for (a) $\lambda_{\text{exi}} = 375$ nm, (b) $\lambda_{\text{exi}} = 405$ nm and (c) $\lambda_{\text{exi}} = 445$ nm.

nm. These data show that the probe molecule at first associates with the micelles and resides at the micellar interface near the AOT headgroups. With gradual increase of the water content in the reverse micelles, the size of micelles increase and as a result the dye molecule migrates to the centre of the water pool from the interface region. The diffusion coefficient parameter (D_w) was calculated using eqn (13), it is a measure of freedom of the wobbling motion. The magnitude of D_w gradually increases at higher w_0 values when $\lambda_{\text{exi}} = 375$ and 405 nm, indicating that the wobbling motion is free at a larger micelles size. The translational (lateral) diffusion coefficient parameter (D_L) also

changes with variation of the w_0 value. Therefore, we observed that at higher w_0 values, with increasing the mobility of the probe molecules, D_w , D_L , θ parameter increases and the corresponding order parameter (S) decreases. These results also gets support as evidenced from the literature.⁵³ From these results we have found a considerable amount of difference in the wobbling-in-cone model parameter with change in the excitation wavelengths ($\lambda_{\text{exi}} = 375$, 405 and 445 nm). The overlay of fluorescence anisotropy decays at different excitation wavelengths in reverse micelles is shown in Fig. 6. Most recently, our group reported a similar kind of excitation wavelength

Table 3 Wobbling-in-cone model parameters for the anisotropy decays of 7-DCCAE in isoctane/water/AOT reverse micelles at different excitation wavelengths

Sr no.	w_0 (nm)	λ_{exi} (nm)	d_{wp} (nm)	r_h (nm)	τ_M (ns)	τ_L (ns)	$D_L = (r_h)^2/(6\tau_L)$ ($10^{-6} \text{ cm}^2 \text{ s}^{-1}$)	S	D_w ($\times 10^{-8}$) (s^{-1})	θ°	τ_w (ns)
1	3	375	1.97	1.985	3.77	3.10	2.12	0.84	2.56	27.22	0.24
2	5		2.55	2.275	5.68	1.97	4.38	0.78	2.92	32.29	0.29
3	10		4	3	13.02	0.97	15.46	0.79	1.61	31.48	0.19
4	20		6.9	4.45	42.49	0.83	39.76	0.70	3.51	38.32	0.32
5	30		9.8	5.9	99.04	0.77	75.35	0.71	4.95	37.60	0.22
6	3	405	1.97	1.985	3.77	5.90	1.11	0.92	1.58	18.97	0.23
7	5		2.55	2.275	5.68	1.67	3.46	0.94	1.25	16.37	0.16
8	10		4	3	13.02	1.06	14.15	0.91	2.51	20.16	0.12
9	20		6.9	4.45	42.49	0.73	45.21	0.87	3.98	24.40	0.13
10	30		9.8	5.9	99.04	0.66	87.90	0.85	5.80	26.31	0.10
11	3	445	1.97	1.985	3.77	9.15	0.72	0.99	0.40	6.63	0.09
12	5		2.55	2.275	5.68	4.07	2.12	0.96	2.05	13.32	0.07
13	10		4	3	13.02	2.25	6.67	0.96	2.40	13.32	0.06
14	20		6.9	4.45	42.49	1.69	19.53	0.99	0.89	6.63	0.04



dependency of 7-DCCA molecule in isooctane/water/AOT reverse micelles.²⁵

3.4. Similarities and differences in the photophysics of 7-DCCA and 7-DCCA

7-DCCA is a hydrophilic molecule, whereas 7-DCCA is more hydrophobic in character. We have observed considerable differences in the absorption and emission spectral properties, fluorescence lifetime and rotational relaxation time of 7-DCCA with 7-DCCA in reverse micelles. The photophysics of 7-DCCA in reverse micelles was reported by us earlier.²⁵ In reverse micelles we have observed that the absorption and emission peak of 7-DCCA (Table 1) is red shifted as compared to 7-DCCA.²⁵ For both molecules we have observed REES in the reverse micelles and the extent of REES gradually decreases with increasing the w_0 value, although the extent of REES for 7-DCCA is less compared to 7-DCCA in the reverse micelles. This may be due to the presence of a carboxylic group in 7-DCCA. The fluorescence quantum yield value (ϕ_f) of 7-DCCA and 7-DCCA gradually decreases with the gradual addition of water content inside the reverse micelles. This result clearly ascertains that both probe molecules face more polar environment with rising of the water content. The magnitude of ϕ_f of 7-DCCA is higher²⁵ in respective reverse micelles as compared to 7-DCCA. For both molecules the quantum yield values are different at different excitation

wavelengths, this demonstrates the excitation wavelength dependent behaviour of both 7-DCCA and its ester molecule.

In the presence of bulk water, 7-DCCA shows the average decay time (τ_f) 0.146 ns while for 7-DCCA the τ_f value is 0.045 ns. The non-radiative decay rate constant (k_{nr}) of 7-DCCA and 7-DCCA is 6.67 and 22 ns⁻¹ respectively. These results suggest profound difference of the non-radiative emission behaviour and their fluorescence properties of 7-DCCA and 7-DCCA in neat water. The probe molecules entrapped in the reverse micelles core become highly fluorescent and their non-radiative decay rate constants values (k_{nr}) decrease and increase the average decay time (τ_f). With gradual increase of the size of the reverse micelles water pool, the τ_f value of both fluorophores gradually decreases. The average decay time (τ_f) and the corresponding non-radiative rate constants (k_{nr}) values of 7-DCCA²⁵ and 7-DCCA are different at different excitation sources (Table 1). The most interesting difference between the photophysics of 7-DCCA and 7-DCCA is that, in the case of 7-DCCA the solvent relaxation time is very fast and we are unable to detect. In our previous report²⁵ we have reported the solvent relaxation time in the same reverse micelles using 7-DCCA. This is due to the fact that 7-DCCA is more hydrophilic than 7-DCCA, therefore it forms strong H-bonding with the water molecule inside the reverse micelles. This leads to retardation of the solvent relaxation time in the case of 7-DCCA. This is directly proven by the rotational relaxation dynamics of both

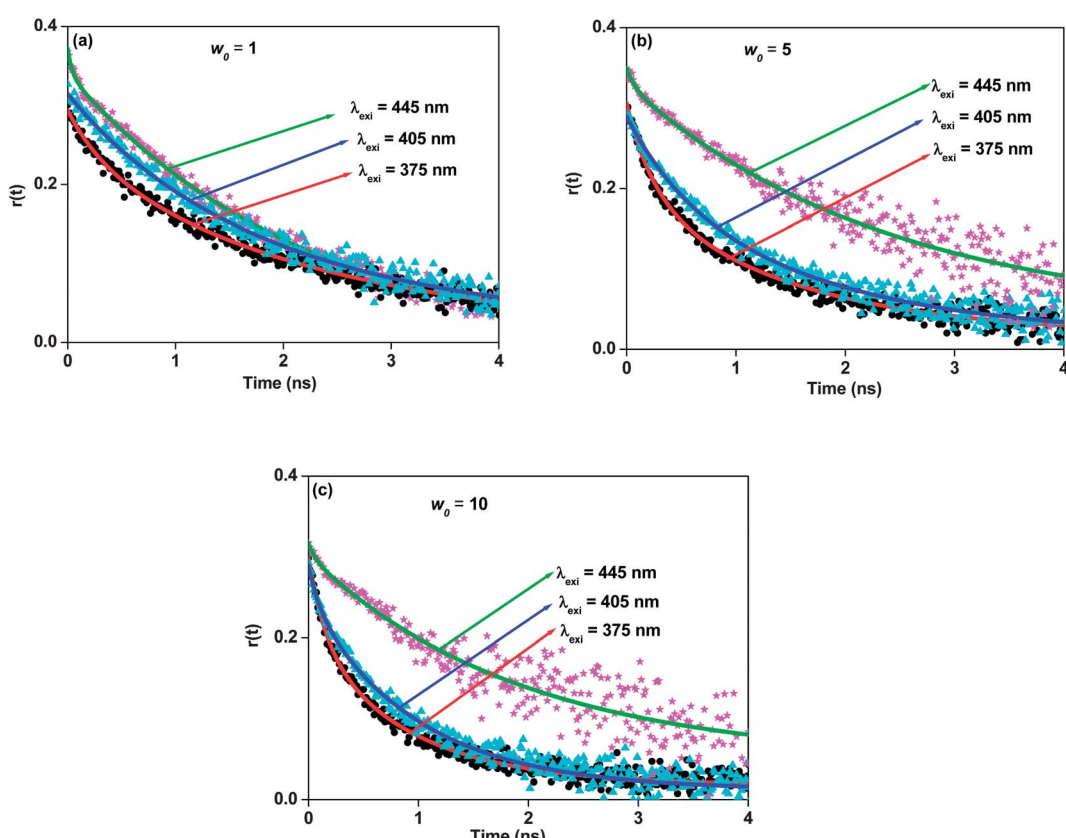


Fig. 6 Difference of fluorescence anisotropy decays of 7-DCCA isoctane/water/AOT reverse micelles at (a) $w_0 = 1$, (b) $w_0 = 5$ and (c) $w_0 = 10$ for $\lambda_{exi} = 375$ nm, $\lambda_{exi} = 405$ nm and $\lambda_{exi} = 445$ nm.

molecules in reverse micelles. We have observed that the average rotational relaxation time of 7-DCCA is always lower than that of 7-DCCA²⁵ in all reverse micelles and different excitation wavelengths. This further proved our statement that 7-DCCA formed more strong H-bonding with the water molecule inside the reverse micelles. This leads to the differences in the photophysics of 7-DCCA with 7-DCCA inside the reverse micelles.

4. Conclusion

The photophysics of 7-(diethylamino)coumarin-3-carboxylic acid *N*-succinimidyl ester (7-DCCA) has been investigated in the presence of aqueous reverse micelles using steady state absorption, fluorescence emission and picosecond time resolved emission spectroscopy. We have found excitation wavelength dependent photodynamics of the dye molecule in this confined medium. We have observed REES of 7-DCCA in reverse micelles. The main reason for such effect may be the specific solute–solvent interaction, such as hydrogen bonding between 7-DCCA with the media. Excitation wavelength dependent excited state dynamics of 7-DCCA was observed in reverse micelles with different w_0 values. With increase in the w_0 value the extent of REES gradually decreases, due to increase of the mobility of the water molecule inside the confined system. The reorientation dynamics of the hydrophobic probe 7-DCCA was explained with the two-step and “wobbling-in-cone model”. The photophysics of 7-DCCA in reverse micelles is quite different from that of 7-DCCA. This is explained with the tendency of the acidic molecule 7-DCCA to form more strong H-bonding with the water molecule inside the reverse micelles as compared to 7-DCCA molecule.

Acknowledgements

D.S. is thankful to IIT Patna, India for research facilities. B.M. is thankful to IIT Patna for research fellowship. A.C. is thankful to IIT Patna and CSIR, New Delhi for research fellowship.

References

- 1 M. P. Pileni, *J. Phys. Chem.*, 1993, **97**, 6961.
- 2 P. L. Luisi, *Adv. Chem. Phys.*, 1996, **92**, 425.
- 3 V. Chhabra, V. Pillai, B. K. Mishra, A. Morrone and D. O. Shah, *Langmuir*, 1995, **11**, 3307.
- 4 A. Kitahara, *Adv. Colloid Interface Sci.*, 1980, **12**, 109.
- 5 M. P. Pileni, *Adv. Colloid Interface Sci.*, 1993, **46**, 139.
- 6 *Structure and Reactivity in Reverse Micelles*, M. P. Pileni, Elsevier, Amsterdam, 1989, vol. 65.
- 7 *Reverse Micelles*, P. L. Luisi and B. E. Straub, Plenum Press, New York, 1984.
- 8 N. Nandi, K. Bhattacharyya and B. Bagchi, *Chem. Rev.*, 2000, **100**, 2013.
- 9 K. Bhattacharyya, *Acc. Chem. Res.*, 2003, **36**, 95.
- 10 J. H. Fendler, *J. Phys. Chem.*, 1980, **84**, 1485.
- 11 E. Keh and B. J. Valeur, *J. Colloid Interface Sci.*, 1981, **79**, 465.
- 12 M. Zulauf and H.-F. Eicke, *J. Phys. Chem.*, 1979, **83**, 480.
- 13 K. Mukherjee, D. C. Mukherjee and S. P. Moulik, *Langmuir*, 1993, **9**, 1727.
- 14 E. Bardez, N. C. Vy and T. Zemb, *Langmuir*, 1995, **11**, 3374.
- 15 T. K. Jain, M. Varshney and A. Maitra, *J. Phys. Chem.*, 1989, **93**, 7409.
- 16 A. Amararene, M. Gindre, J.-Y. Le Huerou, C. Nicot, W. Urbach and M. Waks, *J. Phys. Chem. B*, 1997, **101**, 10751.
- 17 H. Hausier, G. Haering, A. Pande and P. L. Luisi, *J. Phys. Chem.*, 1989, **93**, 7869.
- 18 S. P. Moulik and B. K. Pal, *Adv. Colloid Interface Sci.*, 1998, **78**, 99.
- 19 S. Vajda, R. Jimenez, S. J. Rosenthal, V. Fidler, G. R. Fleming and E. W. Castner Jr, *J. Chem. Soc., Faraday Trans.*, 1995, **91**, 867.
- 20 N. Sarkar, A. Datta and K. Bhattacharyya, *J. Phys. Chem.*, 1996, **100**, 15483.
- 21 P. Hazra, D. Chakrabarty and N. Sarkar, *Langmuir*, 2002, **18**, 7872.
- 22 R. E. Riter, E. P. Undiks and N. E. Levinger, *J. Am. Chem. Soc.*, 1998, **120**, 6062.
- 23 R. E. Riter, D. M. Willard and N. E. Levinger, *J. Phys. Chem. B*, 1998, **102**, 2705.
- 24 D. M. Willard and N. E. Levinger, *J. Phys. Chem. B*, 2000, **104**, 11075.
- 25 A. Chatterjee, B. Maity and D. Seth, *Phys. Chem. Chem. Phys.*, 2013, **15**, 1894.
- 26 Q. Lin, C. Bao, G. Fan, S. Cheng, H. Liu, Z. Liu and L. Zhu, *J. Mater. Chem.*, 2012, **22**, 6680.
- 27 A. Hong and J. He, *J. Biomol. Tech.*, 2010, **21**, 45.
- 28 L. Heide, *Methods Enzymol.*, 2009, **459**, 437.
- 29 M. Ehrbar, R. Schoenmakers, E. H. Christen, M. Fussenegger and W. Weber, *Nat. Mater.*, 2008, **7**, 800.
- 30 A. N. Fletcher, *Appl. Phys.*, 1977, **14**, 295.
- 31 R. L. Atkins and D. E. Bliss, *J. Org. Chem.*, 1978, **43**, 1975.
- 32 C. R. Moylan, *J. Phys. Chem.*, 1994, **98**, 13513.
- 33 T. L. Arbeloa, F. L. Arbeloa, M. J. Tapia and I. L. Arbeloa, *J. Phys. Chem.*, 1993, **97**, 4704.
- 34 G. Jones II, W. R. Jackson, C. Y. Choi and W. R. Bergmark, *J. Phys. Chem.*, 1985, **89**, 294.
- 35 M. R. Webb and J. E. T. Corrie, *Biophys. J.*, 2001, **81**, 1562.
- 36 J. M. Arguello and J. H. Kaplan, *J. Biol. Chem.*, 1994, **269**, 6892.
- 37 T. Higashijima, T. Fuchigami, T. Imasaka and N. Ishibashi, *Anal. Chem.*, 1992, **64**, 711.
- 38 V. Chechik, *Annu. Rep. Prog. Chem., Sect. B*, 2006, **102**, 357.
- 39 S. Sakamoto and K. Kudo, *J. Am. Chem. Soc.*, 2008, **130**, 9574.
- 40 A. K. Mandal, D. K. Das, A. K. Das, S. S. Mojumdar and K. Bhattacharyya, *J. Phys. Chem. B*, 2011, **115**, 10456.
- 41 A. Chatterjee and D. Seth, *Photochem. Photobiol.*, 2013, **89**, 280.
- 42 V. G. Rao, C. Ghatak, R. Pramanik, S. Sarkar and N. Sarkar, *J. Phys. Chem. B*, 2011, **115**, 10500.
- 43 C. Banerjee, S. Mandal, S. Ghosh, V. G. Rao and N. Sarkar, *J. Phys. Chem. B*, 2012, **116**, 11313.
- 44 K. Bhattacharyya, *Chem. Commun.*, 2008, 2848–2857.
- 45 S. Balasubramanian, S. Pal and B. Bagchi, *Phys. Rev. Lett.*, 2002, **89**, 115505-1.



- 46 A. K. Satpati, M. Kumbhakar, S. Nath and H. Pal, *ChemPhysChem*, 2009, **10**, 2966.
- 47 E. M. Corbeil, R. E. Riter and N. E. Levinger, *J. Phys. Chem. B*, 2004, **108**, 10777.
- 48 H. Shirota and K. Horie, *J. Phys. Chem. B*, 1999, **103**, 1437.
- 49 P. Hazra and N. Sarkar, *Chem. Phys. Lett.*, 2001, **342**, 303.
- 50 J. R. Lakowicz, *Principles of Fluorescence Spectroscopy*, Springer, New York, 3rd edn, 2006, p. 54.
- 51 E. L. Quitevis, A. H. Marcus and M. D. Fayer, *J. Phys. Chem.*, 1993, **97**, 5762.
- 52 G. Lipari and A. Szabo, *Biophys. J.*, 1980, **30**, 489.
- 53 G. Lipari and A. Szabo, *J. Am. Chem. Soc.*, 1982, **104**, 4546.
- 54 N. C. Maity, S. Mazumdar and N. Periasamy, *J. Phys. Chem.*, 1995, **99**, 10708.
- 55 N. C. Maity, M. M. G. Krishna, P. J. Britto and N. Periasamy, *J. Phys. Chem. B*, 1997, **101**, 11051.
- 56 A. Chakraborty, D. Seth, P. Setua and N. Sarkar, *J. Phys. Chem. B*, 2006, **110**, 5359.
- 57 G. B. Dutt, *Langmuir*, 2005, **21**, 10391.
- 58 G. B. Dutt, *J. Phys. Chem. B*, 2002, **106**, 7398.
- 59 G. B. Dutt, *J. Phys. Chem. B*, 2008, **112**, 7220.
- 60 A. S. Klymchenko and A. P. Demchenko, *J. Am. Chem. Soc.*, 2002, **124**, 12372.
- 61 P. K. Mandal, M. Sarkar and A. Samanta, *J. Phys. Chem. A*, 2004, **108**, 9048.
- 62 A. P. Demchenko, *Luminescence*, 2002, **17**, 19.
- 63 J. R. Lakowicz and S. K. Nakamoto, *Biochemistry*, 1984, **23**, 3013.
- 64 A. Chattopadhyay, S. Mukherjee and H. Raghuraman, *J. Phys. Chem. B*, 2002, **106**, 13002.
- 65 R. D. Ludescher, L. Peting, S. Hudson and B. Hudson, *Biophys. Chem.*, 1987, **28**, 59.
- 66 B. Bhattacharya, S. Nakka, L. Guruprasad and A. Samanta, *J. Phys. Chem. B*, 2009, **113**, 2143.

